Contribution from the Department of Chemistry, The Ohio State University, Columbus, Ohio 43210, and Molecular Structure Center, Department of Chemistry, Indiana University, Bloomington, Indiana 47405

Irida-, Rhoda-, Nickela-, and Cuprapentaboranes Derived from the *arachno*-$[B_4H_9]^-$ Ion. Crystal Structure of $[Ir(\eta^4\text{-}B_4H_9)(CO)\{P(CH_3)_2C_6H_5\}_2]$, an Analogue of *arachno*-B_5H_{11} and $[Ir(\eta^4\text{-}C_4H_6)(CO)\{P(CH_3)_2C_6H_5\}_2]^+$

SIMON K. BOOCOCK,† MARK A. TOFT,† KENNETH E. INKROTT,† LEH-YEH HSU,† JOHN C. HUFFMAN,‡ KIRSTEN FOLTING,‡ and SHELDON G. SHORE*†

Received November 29, 1983

The reaction of $K[B_4H_9]$ with *trans*-$[IrCl(CO)\{P(CH_3)_2C_6H_5\}_2]$, $[RhCl\{P(C_6H_5)_3\}_3]$, $[NiBr_2\{(C_6H_5)_2P(CH_2)_2P(C_6H_5)_2\}]$ (in the presence of an additional 1 equiv of KH), and $[CuBr\{P(C_6H_5)_3\}_2 \cdot {}^1/_2C_6H_6]$ yields respectively $[Ir(\eta^4\text{-}B_4H_9)(CO)\{P(CH_3)_2C_6H_5\}_2]$ (I), $[Rh(\eta^3\text{-}B_4H_8)H\{P(C_6H_5)_3\}_2]$ (II), $[Ni(\eta^3\text{-}B_4H_8)\{(C_6H_5)_2P(CH_2)_2P(C_6H_5)_2\}]$ (III), and $[Cu(\eta^3\text{-}B_4H_9)\{P(C_6H_5)_3\}_2]$ (IV). Boron-11 and $^1H\{^{11}B\}$ NMR spectroscopies were used to characterize these metallapentaboranes. Complex I crystallized from pentane at −20 °C as colorless needles; the crystal structure of $[Ir(\eta^4\text{-}B_4H_9)(CO)\{P(CH_3)_2C_6H_5\}_2]$ was determined. Crystal parameters: space group $P2_1/c$, $a = 9.324$ (2) Å, $b = 23.162$ (10) Å, $c = 12.286$ (3) Å, $\beta = 55.95$ (1)°, $V = 2198.5$ Å^3, $Z = 4$, mol wt = 548.84, $\rho_c = 1.658$ g cm^{-3}, $\mu_c = 61.989$ cm^{-1} for Mo Kα. The structure analysis is based upon 3159 independent reflections with $F > 2.33\sigma(F)$ collected on a Picker four-circle diffractometer, the range being $5° \le 2\theta \le 50°$ at −162 ± 4 °C. Final $R(F) = 0.054$ and $R_w(F) = 0.050$. In the crystalline state complex I has C_i symmetry. The molecule consists of an open five-atom cluster in which the $[Ir(CO)\{P(CH_3)_2C_6H_5\}_2]$ fragment occupies an apical vertex site and is bound to the four boron atoms of the $[\eta^4\text{-}B_4H_9]$ ligand. Complex I is an analogue of *arachno*-B_5H_{11} and the $[Ir(\eta^4\text{-}C_4H_6)(CO)\{P(CH_3)_2C_6H_5\}_2]^+$ cation.

Introduction

The development of a simple synthesis of B_4H_{10}[1] has made available a potentially convenient route to metallapentaboranes by reaction of the $[B_4H_9]^-$ ion with suitable transition-metal complexes. The $[B_4H_9]^-$ ion is readily prepared from B_4H_{10} by deprotonation, typically with KH, in etheric solution.[2] Although metallapentaboranes have been known for some years, they have, in general, been synthesized by indirect methods from either higher boron hydrides or borane anions other than $[B_4H_9]^-$.[3-10,54] We now report the synthesis and characterization of four metallapentaboranes derived from $[B_4H_9]^-$ via B_4H_{10}: $[Ir(\eta^4\text{-}B_4H_9)(CO)\{P(CH_3)_2C_6H_5\}_2]$ (I), $[Rh(\eta^3\text{-}B_4H_8)H\{P(C_6H_5)_3\}_2]$ (II), $[Ni(\eta^3\text{-}B_4H_8)\{(C_6H_5)_2P(CH_2)_2P(C_6H_5)_2\}]$ (III), and $[Cu(\eta^3\text{-}B_4H_9)\{P(C_6H_5)_3\}_2]$ (IV). These exhibit three structural types (vide infra). Compound IV has been the subject of a preliminary report;[11] we also now report some details of the methyl-substituted analogue of IV, $[Cu(\eta^3\text{-}4\text{-}CH_3B_4H_8)\{P(C_6H_5)_3\}_2]$ (V).[10]

The iridium complex $[Ir(\eta^4\text{-}B_4H_9)(CO)\{P(CH_3)_2C_6H_5\}_2]$ deserves special attention because, of the metallapentaboranes derived from B_4H_{10}, this is the only example for which a similar compound, $[Ir(\eta^4\text{-}B_4H_9)(CO)\{P(CH_3)_3\}_2]$ (VI), has been prepared by an indirect method.[10] The yield of VI is low. This is a general feature of less direct synthetic routes to metallapentaboranes. The synthetic strategies outlined within this paper might be applied to an attempt to obtain the previously known examples of metallapentaboranes in more favorable yields or larger quantities.

Results and Discussion

$[Ir(\eta^4\text{-}B_4H_9)(CO)\{P(CH_3)_2C_6H_5\}_2]$ (I). The iridaborane complex I is conveniently prepared by the reaction of *trans*-$[IrCl(CO)\{P(CH_3)_2C_6H_5\}_2]$ with $K[B_4H_9]$ according to eq 1. Complex I can be isolated as a white air-stable solid

$$[IrCl(CO)\{P(CH_3)_2C_6H_5\}_2] + K[B_4H_9] \xrightarrow[-18\ °C]{THF/CH_2Cl_2} \underset{I}{[Ir(\eta^4\text{-}B_4H_9)(CO)\{P(CH_3)_2C_6H_5\}_2]} + KCl \quad (1)$$

by thin-layer chromatography on silica gel in 60–70% yield. It is soluble in a wide range of aromatic and aliphatic solvents and can be recrystallized from hexane or pentane.

Table I. Selected Interatomic Distances (Å) for $[1,1,1\text{-}(CO)(PMe_2Ph)_2(1\text{-}IrB_4H_9)]$

Ir(1)-P(8)	2.365 (3)	B(5)-B(4)	1.852 (20)
Ir(1)-P(9)	2.340 (3)	B(4)-B(3)	1.828 (20)
Ir(1)-C(6)	1.911 (11)	B(2)-H(1)	0.94 (9)
Ir(1)-B(2)	2.226 (13)	B(2)-H(3)	1.29 (18)
Ir(1)-B(3)	2.258 (12)	B(5)-H(4)	1.19 (9)
Ir(1)-B(4)	2.154 (12)	B(5)-H(5)	1.24 (14)
Ir(1)-B(5)	2.147 (14)	B(4)-H(8)	1.23 (9)
B(2)-B(3)	1.855 (19)	B(3)-H(9)	1.13 (10)
B(2)-H(2)[a]	1.33 (12)	B(4)-H(7)[a]	1.23 (9)
B(3)-H(2)[a]	1.19 (11)	B(4)-H(6)[a]	1.42 (13)
B(3)-H(7)[a]	1.29 (8)	B(5)-H(3)[a]	1.35 (13)

[a] Bridging hydrogens.

Table II. Selected Angles (deg) between Interatomic Vectors for $[1,1,1\text{-}(CO)(PMe_2Ph)_2(1\text{-}IrB_4H_9)]$

P(8)-Ir(1)-P(9)	100.7 (1)	B(2)-Ir(1)-B(5)	85.5 (5)
P(8)-Ir(1)-C(6)	89.8 (3)	B(3)-Ir(1)-B(4)	50.3 (5)
P(9)-Ir(1)-C(6)	97.2 (3)	B(3)-Ir(1)-B(5)	87.1 (5)
P(8)-Ir(1)-B(2)	170.4 (3)	B(4)-Ir(1)-B(5)	49.6 (5)
P(9)-Ir(1)-B(2)	97.2 (3)	Ir(1)-B(2)-B(3)	62.7 (6)
C(6)-Ir(1)-B(2)	90.5 (5)	Ir(1)-B(3)-B(2)	67.1 (6)
P(8)-Ir(1)-B(2)	93.8 (4)	Ir(1)-B(3)-B(4)	65.0 (6)
P(9)-Ir(1)-B(5)	84.7 (3)	Ir(1)-B(4)-B(3)	64.7 (6)
C(6)-Ir(1)-B(5)	175.6 (5)	Ir(1)-B(4)-B(5)	68.1 (5)
P(8)-Ir(1)-B(3)	120.3 (4)	B(2)-B(3)-B(4)	107.0 (10)
P(9)-Ir(1)-B(3)	138.7 (4)	B(5)-B(4)-B(3)	111.3 (9)
C(6)-Ir(1)-B(3)	88.8 (5)	Ir(1)-B(2)-H(1)	119 (6)
P(8)-Ir(1)-B(4)	87.2 (3)	Ir(1)-B(2)-H(2)	101 (5)
P(9)-Ir(1)-B(4)	134.1 (4)	Ir(1)-B(2)-H(3)	104 (7)
C(6)-Ir(1)-B(4)	128.2 (5)	B(3)-B(2)-H(1)	115 (5)
B(2)-Ir(1)-B(3)	50.3 (5)	B(3)-B(2)-H(2)	40 (5)
B(2)-Ir(1)-B(4)	85.0 (5)	B(3)-B(2)-H(3)	105 (8)

The molecular structure of I was determined by a single-crystal X-ray diffraction study and is shown in Figure 1.

(1) Leach, J. B.; Toft, M. A.; Himpsl, F. L.; Shore, S. G. *Inorg. Chem.* **1982**, *21*, 1952.
(2) Remmel, R. J.; Johnson, H. D., II; Jaworisky, I. S.; Shore, S. G. *J. Am. Chem. Soc.* **1975**, *97*, 5395.
(3) Greenwood, N. N.; Savory, C. G.; Grimes, R. N.; Sneddon, L. G.; Davison, A.; Wreford, S. S. *J. Chem. Soc., Chem. Commun.* **1974**, 718.
(4) Fehlner, T. P.; Ragaini, J. D.; Mangion, M.; Shore, S. G. *J. Am. Chem. Soc.* **1976**, *98*, 7085.
(5) Shore, S. G.; Ragaini, J. D.; Smith, R. L.; Cottrell, C. E.; Fehlner, T. P. *Inorg. Chem.* **1979**, *18*, 670.
(6) Gaines, D. F.; Hildebrant, S. J. *Inorg. Chem.* **1978**, *17*, 794.
(7) Miller, V. R.; Grimes, R. N. *J. Am. Chem. Soc.* **1976**, *98*, 1600.

† The Ohio State University.
‡ Indiana University.

0020-1669/84/1323-3084$01.50/0

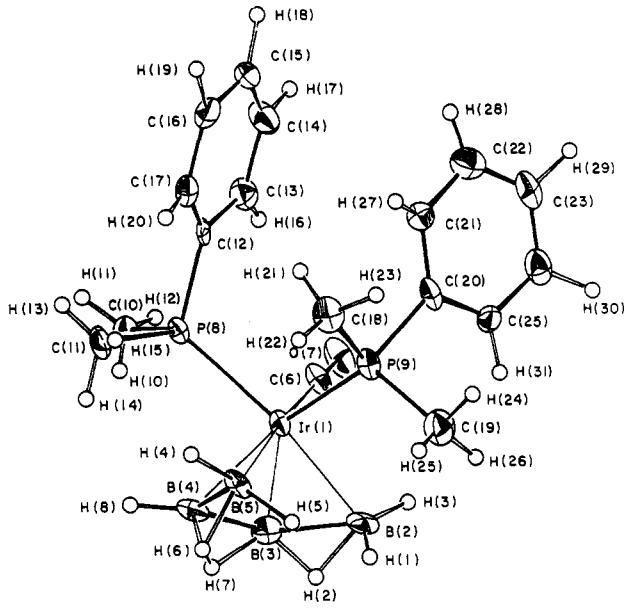

Figure 1. Molecular structure of $[Ir(\eta^4\text{-}B_4H_9)(CO)\{P(CH_3)_2C_6H_5\}_2]$.

(Selected interatomic distances and angles between bonding vectors are shown in Tables I and II.)

The structure is based upon an idealized open four-sided pyramidal arrangement of an *arachno*-$[IrB_4]$ cluster. The parent borane species is B_5H_{11}. Complex I is also isoelectronic with the 1,3-butadiene complex cation[12] $[Ir(\eta^4\text{-}C_4H_6)(CO)\{P(CH_3)_2C_6H_5\}_2]^+$.[12]

Due to the orientation of the neutral ligands about the apical iridium atom, complex I has C_1 rather than C_s symmetry. The iridium atom links to two $P(CH_3)_2C_6H_5$ ligands and one terminal carbonyl group. The boron atoms B(2) and B(5) bond to two terminal and two bridging hydrogen atoms, while the boron atoms B(3) and B(4) link to one terminal and two bridging hydrogen atoms, one of which is shared between the two B–H groups. Phosphorus atom P(8) is trans to B(2) with B(2)–Ir(1)–P(8) = 170.4 (3°) and is displaced on the closed side of the cluster; the other phosphine resides on the open side of the IrB_4 cluster. The terminal carbonyl is trans to the B(5) atom with the angle B(5)–Ir(1)–C(6) = 175.6 (5)°. Boron–iridium bond distances (2.147 (14)–2.258 (12) Å) compare well with those in the other small iridium–boron cluster studied by X-ray diffraction.[13] Boron–boron bond distances in the $[B_4H_9]$ ligand at 1.828 (20)–1.855 (19) Å correspond well to distances in B_5H_{11}.[14] In fact the $[B_4H_9]$ unit can be almost perfectly superimposed upon the array of basal boron atoms in *arachno*-B_5H_{11} (see Figure 2). The boron–boron bond distances are somewhat longer than those found in either $[Co(\eta^3\text{-}B_4H_8)(\eta^5\text{-}C_5H_5)]$[15] or $[Cu(B_5H_8)\{P(C_6H_5)_3\}_2]$,[16] on the order of 0.10–0.20 Å. This phenomenon is probably a direct consequence of the fact that the iridaborane adopts the more

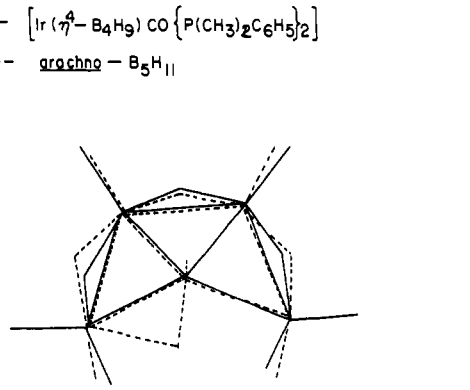

Figure 2. Superimposition of *arachno*-B_5H_{11} upon $[Ir(\eta^4\text{-}B_4H_9)(CO)\{P(CH_3)_2C_6H_5\}_2]$.

open structure of a arachno borane, rather than the nido borane structures exhibited by the cobalta- and cupraboranes cited above.

According to Wade's[17,18] rules of electron counting, the iridaborane complex can be classified as an arachno metallaborane analogue of B_5H_{11} and an analogue of the 1,3-butadiene complex $[Ir(\eta^4\text{-}C_4H_6)(CO)\{P(CH_3)_2C_6H_5\}_2]^+$.[12] These electron-counting rules do not however allow one to assign a formal oxidation state to the metal atom. Two independent approaches may be considered; they assign different values to the formal oxidation state.

Either one considers the complex to be a derivative of $[B_4H_9]^-$ or of the hypothetical borane anion $[B_4H_9]^{3-}$. In the former case the iridium atom and its associated ligands act as a capping vertex, $[Ir^I(CO)(PR_3)_2]^+$. The iridum atom will thus donate two electrons to the cluster. This with the seven electron pairs from $[B_4H_9]^-$ gives a total of eight electron pairs. There are five vertices; hence, the electron pair count is $n + 3$ (where n is the number of vertices), consistent with a five-vertex arachno metallaborane.[17,18] Using such an approach, one may consider the complex as being the borane analogue of the 1,3-butadiene complex $[Ir^I(\eta^4\text{-}C_4H_6)(CO)(PR_3)_2]^+$[12] (1,3-butadiene is isoelectronic with $[B_4H_9]^-$).

In the second case the problem is approached by regarding the structure of B_5H_{11}.[14] The $[B_4H_9]$ ligand found in complex I can be formally generated from B_5H_{11} by the removal of the apical BH group and its attached bridging proton.[14,17,18] Typically in such a formal transformation one views the removed boron vertex, BH, as carrying a double positive charge.[17,18] For instance in just this manner one can remove BH^{2+} from the *closo*-$[B_6H_6]^{2-}$ anion, generating the hypothetical *nido*-$[B_5H_5]^{4-}$ anion. Formal protonation of this species gives *nido*-B_5H_9. Hence the removal of BH^{2+} and H^+ from *arachno*-B_5H_{11} will result in the formation of the hypothetical *hypho*-$[B_4H_9]^{3-}$ anion. Thus in the iridaborane I the $[Ir(CO)\{P(CH_3)_2C_6H_5\}_2]^{3+}$ unit will contribute one vertex but *no* additional bonding electrons to the $[B_4H_9]^{3-}$ anion.

These approaches suggest a dichotomy wherein one can consider the iridium atom as being in either a 3+ or a 1+ formal oxidation state. This is similar to the case of the formal representations of the bonding for 1,3-butadiene complexes such as $[(\eta^4\text{-}C_4H_6)Fe(CO)_3]$.[19]

Spectra. **^{11}B NMR.** The ^{11}B NMR spectrum of complex I at 28.87 MHz and 87 °C consists of a doublet and a triplet of equal intensities, read from low to high field (Figure 3a). This is taken to be due to the presence of two BH and two BH_2 groups in a $[B_4H_9]$ ligand of C_s symmetry. Upon recording the ^{11}B NMR spectrum of I at 96.28 MHz and 25 °C however, one observes that the low-field doublet has become split into

(8) Miller, V. R.; Weiss, R.; Grimes, R. N. *J. Am. Chem. Soc.* **1977**, *99*, 5646.
(9) Weiss, R.; Bowser, J. R.; Grimes, R. N. *Inorg. Chem.* **1978**, *17*, 1522.
(10) Bould, J.; Greenwood, N. N.; Kennedy, J. D. *J. Chem. Soc., Dalton Trans.* **1982**, 481.
(11) Inkrott, K. E.; Shore, S. G. *J. Chem. Soc., Chem. Commun.* **1978**, 866.
(12) Shaw, B. L.; Deeming, A. J. *J. Chem. Soc. A* **1971**, 376.
(13) Greenwood, N. N.; Kennedy, J. D.; McDonald, W. S.; Reed, D.; Staves, J. *J. Chem. Soc., Dalton Trans.* **1979**, 117.
(14) Huffman, J. C. Ph.D. Dissertation, Indiana University, Bloomington, IN, 1974. This represents a redetermination of the structure of B_5H_{11} from diffractometer data. The structure was originally determined from photographic data: Lavine, L.; Lipscomb, W. N. *J. Chem. Phys.* **1954**, *22*, 614. Dickerson, R. E.; Lipscomb, W. N. *Ibid.* **1957**, *27*, 209.
(15) Sneddon, L. G.; Voet, D. *J. Chem. Soc., Chem. Commun.* **1976**, 118.
(16) Brice, V. T.; Shore, S. G. *J. Chem. Soc.* **1975**, 334. Greenwood, N. N.; Howard, J. A.; McDonald, W. S. *J. Chem. Soc., Dalton Trans.* **1977**, 37.
(17) Wade, K. *Adv. Inorg. Chem. Radiochem.* **1976**, *18*, 1.
(18) Wade, K., *Chem. Br.* **1975**, *11*, 177.
(19) Cotton, F. A.; Wilkinson, G. "Advanced Inorganic Chemistry", 4th ed.; Wiley-Interscience: New York, 1980; p 98.

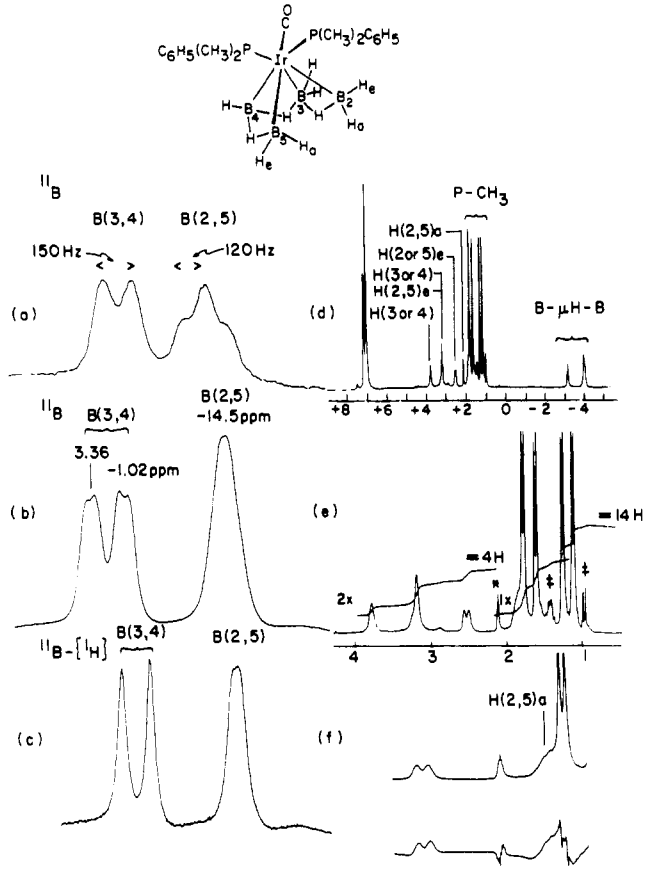

Figure 3. NMR spectra of $[Ir(\eta^4\text{-}B_4H_9)(CO)\{P(CH_3)_2C_6H_5\}_2]$. (a) 28.87-MHz ^{11}B NMR spectrum of I at 87 °C. (b) 96.28-MHz ^{11}B NMR spectrum of I at 25 °C. (c) 96.28-MHz ^{11}B{^{1}H} NMR spectrum of I at 25 °C. (d) 300-MHz ^{1}H{^{11}B} NMR spectrum of I at −45 °C. (e) An expansion of the terminal boron hydride proton resonances from d, where * denotes the resonance due to $C_6D_5C^1HD_2$ and ‡ denotes alkane impurities. (f) Subtraction of the *P*-methyl proton resonance from the ^{1}H{^{11}B} (300-MHz) NMR spectrum of I, showing the remaining boron hydride resonance buried beneath the *P*-methyl resonance.

two doublets each of intensity 1 (Figure 3b) with respect to a broad unresolved resonance of intensity 2 at high field.

These ^{11}B NMR spectra are consistent with a site-exchange process, via mutual pseudorotation, resulting in the averaging of the pairs of boron sites B(3) ⇄ B(4) and B(2) ⇄ B(5). This process then is fast on the NMR time scale at 87 °C and $\nu(^{11}B)$ = 28.87 MHz but is slow at 25 °C and $\nu(^{11}B)$ = 96.28 MHz. Site exchange via mutual pseudorotation is known for η^4-metallaboranes.[20,21] Further, the ^{11}B NMR spectra, at high field and ambient temperatures, are indicative of an asymmetric limiting solution structure for I. This is not surprising in that the structure of I in the solid state, found by X-ray crystallography, is also asymmetric. The asymmetry in complex I is imposed by the disposition of the neutral ligands on the iridium atom, with respect to the $[B_4H_9]$ ligand.

^{1}H NMR. Under conditions of limiting exchange, if one presumes the complex to be asymmetric as found in the solid state (Figure 1), then one would expect to see nine independent proton resonances attributable to the $[B_4H_9]$ ligand. At −45 °C in toluene-d_8 however one observes six resonances in the ratio 1:2:1:2:1:2 (Figure 3). These are attributable to the different sites in the $[B_4H_9]$ ligand by selective decoupling. The resonance at $\delta(^1H)$ = ca. 1.90 is partially obscured by the $P(CH_3)_2$ group's proton spectrum (Figure 3). Of interest is the resonance at $\delta(^1H)$ = 2.6, which is a doublet. This is attributed to long-range $^3J(^{31}P\text{–}^1H)$ coupling between a phosphorus nucleus and a terminal hydride on B(2) or B(5). Doublet character is partially evident in the resonance at $\delta(^1H)$ = 1.90 and may be the cause of the broad shoulder that comprises a portion of the resonance at $\delta(^1H)$ = 3.20. Such broadening of these resonances, or doublet character, is also attributed to long range $^nJ(^{31}P\text{–}^1H)$ coupling to the protons on boron atoms B(2) and B(5). At elevated temperatures in toluene-d_8 the borane resonances in the $^1H\{^{11}B(\text{broad band})\}$ NMR spectrum simplify to a 2:2:2:1:2 pattern consistent with an averaged structure for the $[B_4H_9]$ ligand produced by site exchange via mutual pseudorotation.

$[Rh(\eta^3\text{-}B_4H_8)H\{P(C_6H_5)_3\}_2]$ (II). The synthesis of II was carried out according to eq 2. The isolated creamy white solid, obtained in 90% yield, exhibits moderate air and thermal stability. This compound is sparingly soluble in CH_2Cl_2 or THF, forming light yellow solutions that decompose with a darkening of color above 0 °C.

$$[RhCl\{P(C_6H_5)_3\}_3] + K[B_4H_9] \xrightarrow[-18\ °C]{THF/CH_2Cl_2} \underset{II}{[Rh(\eta^3\text{-}B_4H_8)H\{P(C_6H_5)_3\}_2]} + KCl + P(C_6H_5)_3 \quad (2)$$

Spectra. IR. The infrared spectrum of the rhodapentaborane is reported in the Experimental Section. Features of interest for the purpose of this discussion include a set of three absorptions at 2300, 2230, and 2160 cm^{-1} (br, w), which are tentatively assigned as M–μ–H–B stretching vibrations,[22,23] and a sharp absorption at 2070 cm^{-1}, which is attributed to an Rh–H_t stretching vibration. The presence of a rhodium hydride is indicative of an oxidative addition of the $[B_4H_9]^-$ ion across the Rh^I atom. Hydrogen is transferred from the $[B_4H_9]^-$ unit onto the rhodium atom, while the rhodium atom becomes incorporated into the resultant $[B_4H_8]$ unit, giving the expanded five-vertex rhodapentaborane. (The presence of a hydride on the rhodium atom is further attested to by the ^{1}H NMR spectra—vide infra.)

NMR. Boron-11 and proton NMR spectra of II are consistent with the four-sided pyramidal arrangement of the four boron atoms and the rhodium atom, which occupies a basal vertex site (Figure 4). In the proton NMR spectrum at 300 MHz the resonances attributable to the borane ligand occur in the ratio 1:1:2:2:2. This indicates that a mirror plane is present in the molecule. The individual borane proton resonances were assigned on the basis of selective decoupling. In addition, resonances due to the phenyl protons and a sharp resonance at $\delta(^1H)$ = −13.33 (assigned to the terminal hydride on the rhodium atom) are observed. The Rh–H–B bridging protons are coupled to the $P(C_6H_5)_3$ ligands on the rhodium atom, as expected from the pseudooctahedral structure shown in Figure 4.

$[Ni(\eta^3\text{-}B_4H_8)\{(C_6H_5)_2P(CH_2)_2P(C_6H_5)_2\}]$ (III). The synthesis of compound III was conducted according to the reaction sequence shown in (3) and (4), where dppe = $(C_6H_5)_2P(CH_2)_2P(C_6H_5)_2$. This synthesis depends upon the strategy of forming an initial intermediate, [NiBr(B$_4$H$_9$)(dppe)], which

$$[NiBr_2(dppe)] + K[B_4H_9] \xrightarrow[-45\ °C]{THF/CH_2Cl_2} [NiBr(B_4H_9)(dppe)] + KBr \quad (3)$$

$$[NiBr(B_4H_9)(dppe)] + KH \xrightarrow[-45\ °C]{THF/CH_2Cl_2} \underset{III}{[Ni(\eta^3\text{-}B_4H_8)(dppe)]} + H_2 + KBr \quad (4)$$

(20) Boocock, S. K.; Greenwood, N. N.; Kennedy, J. D. *J. Chem. Soc., Chem. Commun.* **1980**, 305.
(21) Boocock, S. K.; Greenwood, N. N.; Kennedy, J. D.; McDonald, W. S.; Staves, J. *J. Chem. Soc., Dalton Trans.* **1981**, 2573.
(22) Outerson, G. G.; Brice, V. T.; Shore, S. G. *Inorg. Chem.* **1976**, *15*, 1456.
(23) Gill, J. T.; Lippard, S. J. *Inorg. Chem.* **1975**, *14*, 751.

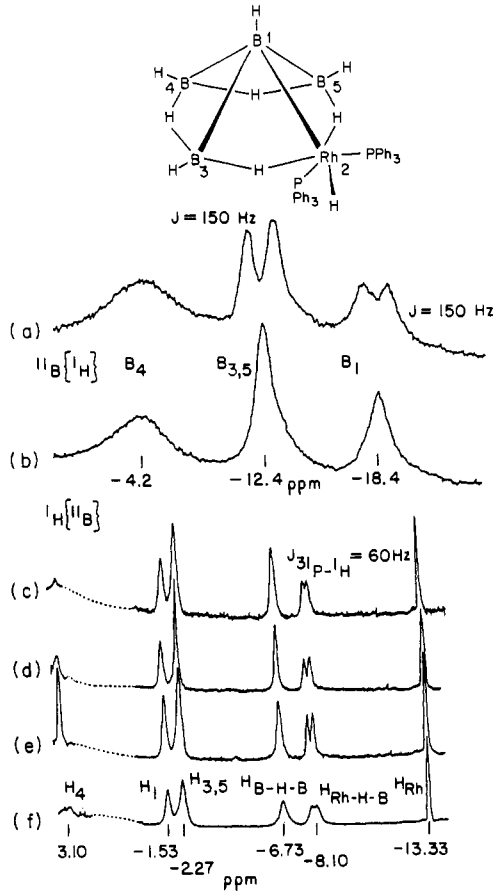

Figure 4. NMR spectra of $[Rh(H)(\eta^3\text{-}B_4H_8)\{P(C_6H_5)_3\}_2]$. (a) ^{11}B NMR spectrum of II at 96.28 MHz and 0 °C in CD_2Cl_2. (b) $^{11}B\{^1H\}$ NMR spectrum of II at 96.28 MHz and 0 °C in CD_2Cl_2. (c–e) $^1H\{^{11}B\}$ selectively decoupled NMR spectra of II at 300 MHz and 0 °C in CD_2Cl_2: c, irradiation at $\nu(^{11}B(1))$; d, irradiation at $\nu(^{11}B(3,5))$; e, irradiation at $\nu(^{11}B(4))$. (f) Broad-band decoupled $^1H\{^{11}B\}$ NMR spectrum of II at 300 MHz and 0 °C in CD_2Cl_2.

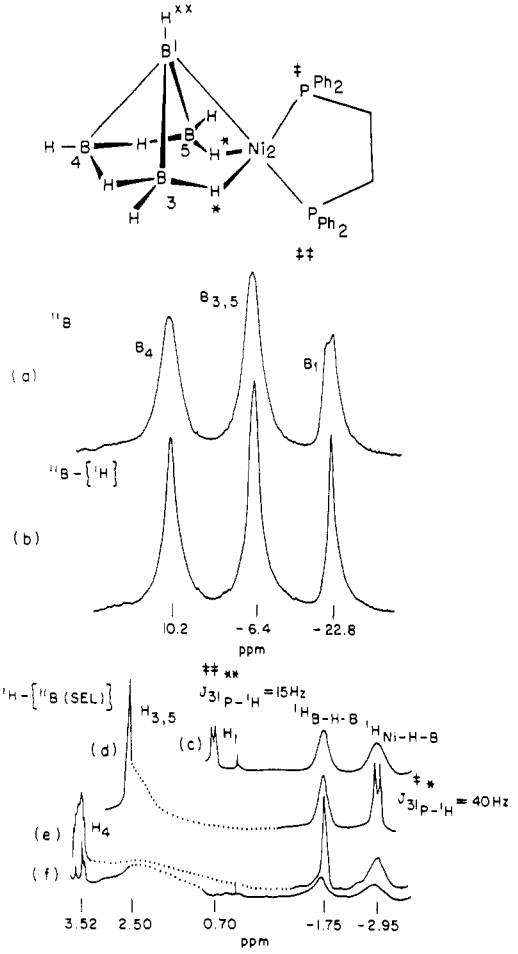

Figure 5. NMR spectra of $[Ni(\eta^3\text{-}B_4H_8)(dppe)]$. (a) ^{11}B NMR spectrum of III at 96.28 MHz and 0 °C in CD_2Cl_2. (b) $^{11}B\{^1H\}$ NMR spectrum of III at 96.28 MHz and 0 °C in CD_2Cl_2. (c–f) $^1H\{^{11}B\}$ NMR spectra of III in CD_2Cl_2 at 0 °C, where * and ** denote the protons coupled to ^{31}P nuclei with notation ‡ and ‡‡, respectively: c, selectively decoupled irradiation at $\nu(^{11}B(1))$; d, selectively decoupled irradiation at $\nu(^{11}B(3,5))$; e, selectively decoupled irradiation at $\nu(^{11}B(4))$; f, broad-band boron-decoupled ^1H NMR spectrum.

is then deprotonated by KH in situ to produce the $[\mu\text{-NiBr}\{(C_6H_5)_2P(CH_2)_2P(C_6H_5)_2\}B_4H_8]^-$ anion. This anion then undergoes an intramolecular displacement of bromide ion with concomitant formation of the product, III. The red-orange product is obtained after chromatographic separation on silica gel, under an inert atmosphere, in about 25% yield.

Spectra. IR. The infrared spectrum of III, taken as a Nujol mull, exhibits stretching vibrations at 2380, 2280, and 2210 cm^{-1}. They are in the range 2400–2100 cm^{-1}, which is assigned to M–μ–H–B stretching modes in other metallaboranes known to contain M–μ–H–B bridges.[22,23] Further details of the infrared spectrum are contained within the Experimental Section.

NMR. The boron-11 and proton NMR spectra of III are shown in Figure 5; also shown is the proposed structure of the nickelaborane, consistent with these spectra.

The boron-11 NMR spectra show three resonances in the ratio 1:2:1; hence, the molecule contains an $[\eta^3\text{-}B_4H_8]$ ligand with mirror symmetry. The proton NMR spectra are also concordant with a molecule containing a mirror plane of symmetry through the $[B_4H_8]$ ligand. Individual resonances were assigned to positional sites in the $[B_4H_8]$ ligand by selective decoupling (Figure 5). Additional coupling between the phosphorus nuclei and the μ-H(2,3) and μ-H(2,5) bridging protons as well as the H(1) proton were ascribed on the basis of the proposed pseudo-trigonal-bipyramidal structure for III shown in Figure 5.

$[Cu(\eta^3\text{-}B_4H_9)\{P(C_6H_5)_3\}_2]$ (IV) was synthesized by either of the two methods shown in eq 5 and 6. The yield of complex IV is 30% in (5) and 51% in (6). It is a white air-stable solid that decomposes in CH_2Cl_2 solution above 0 °C.

$$[CuCl\{P(C_6H_5)_3\}_3] + K[B_4H_9] \xrightarrow[-45\ °C]{THF/CH_2Cl_2} [Cu(\eta^3\text{-}B_4H_9)\{P(C_6H_5)_3\}_2] + KCl + P(C_6H_5)_3 \quad (5)$$
IV

$$[CuBr\{P(C_6H_5)_3\}_2\cdot{}^1/_2C_6H_6] + K[B_4H_9] \xrightarrow[-45\ °C]{THF/CH_2Cl_2} [Cu(\eta^3\text{-}B_4H_9)\{P(C_6H_5)_3\}_2] + KBr + {}^1/_2C_6H_6 \quad (6)$$
IV

Spectra. The ^{11}B and $^{11}B\{^1H\}$ NMR spectra of IV were recorded at −20 °C in CD_2Cl_2 at 96.27 MHz. They are shown in Figure 6. The triplet assigned to B(1) has a chemical shift of −55.8 ppm. There are also two resonances of relative intensity 1:2 at $\delta(^{11}B)$ = +1.6 and −6.5, respectively. The resonance at −6.5 ppm clearly exhibits coupling with two protons (J = 110 Hz). The resonance at +1.6 ppm does not show any proton coupling but does sharpen on broad-band decoupling from protons.

The $^1H\{^{11}B$ decoupled$\}$ NMR spectra of the cuprapentaborane (Figure 6), between the temperatures −66 and 0 °C, are consistent with those obtained for the limiting exchange of the $[B_4H_9]^-$ ion at −100 °C.[2] Whereas the free $[B_4H_9]^-$ ion exhibits dynamic behavior at higher temperatures (e.g., −50 °C), indicating exchange of protons between bridging and

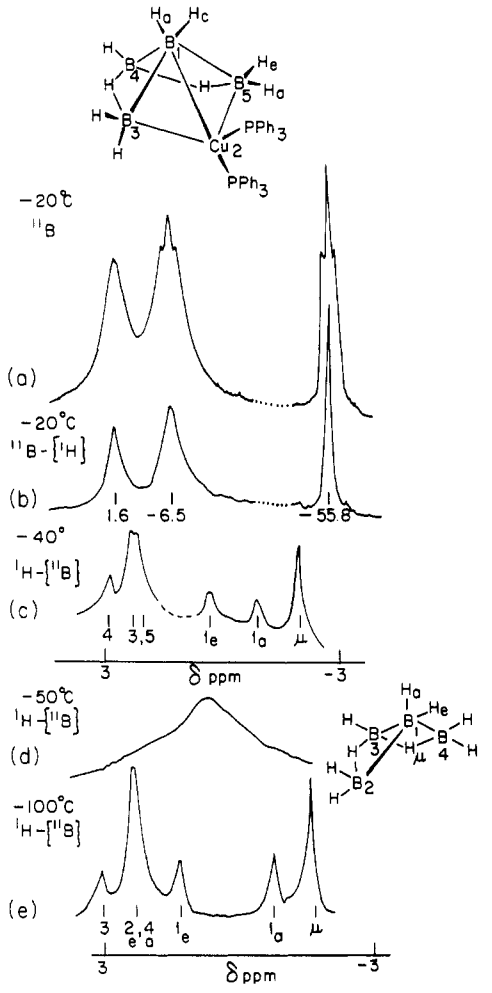

Figure 6. NMR spectra of $[Cu(\eta^3\text{-}B_4H_9)\{P(C_6H_5)_3\}_2]$ and $K[B_4H_9]$. (a) ^{11}B NMR spectrum of IV at 96.28 MHz. (b) ^{11}B{^{1}H} NMR spectrum of IV at 96.28 MHz. (c) ^{1}H{^{11}B} (broad-band decoupled) NMR spectrum of IV at 100 MHz. (d) ^{1}H{^{11}B} NMR spectrum of $K[B_4H_9]$ at −50 °C and 100 MHz. (e) ^{1}H{^{11}B} NMR spectrum of $K[B_4H_9]$ at −100 °C and 100 MHz.

terminal sites, within the temperature range −66 to 0 °C $[Cu(B_4H_9)\{P(C_6H_5)_3\}_2]$ shows no evidence for such site exchange. Hence the compound is not a simple salt.

Additional support for this structure (Figure 6) comes from the *lack* of stretching vibrations in the 2400–2100-cm^{-1} region, normally attributed to Cu–μ-H–B stretching modes.[22,23] This would rule out a structure involving Cu–μ-H–B bonding through the axial H atoms on B(3) and B(5) (Figure 7). Typically such an arrangement will also give fluxional systems with ^{1}H NMR spectra that are single broad resonances.[24] Another structural arrangement would contain copper at a bridging site between either B(1) and B(2) or B(2) and B(4) of $[B_4H_9]^-$ (Figure 7). A ^{1}H NMR spectrum suggesting C_s symmetry could be produced by rapid oscillation of the borane framework. The copper atom would then exchange between the two bridging sites. Such an exchange process would be very likely accompanied by concomitant proton exchange. Such a supposition is hardly justified, especially at the highest temperature (0 °C) of the ^{1}H NMR study. The apparent absence of proton-exchange averaging at 0 °C and the absence of evidence for loss of apparent C_s symmetry (through retardation of Cu–borane oscillation) at lower temperatures lead us to consider that this third structural possibility is not likely.

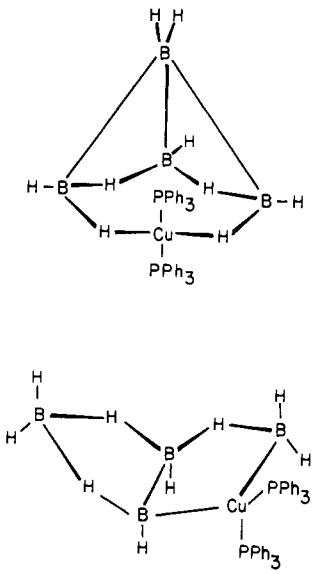

Figure 7. Alternative structural arrangements for IV.

The related complex $[Cu(\eta^4\text{-}4\text{-}CH_3B_4H_8)\{P(C_6H_5)_3\}_2]$ can be synthesized in an analogous manner from $K[1\text{-}CH_3B_4H_8]$. The 28.87 MHz ^{11}B NMR spectrum of complex V shows three resonances with relative areas 1:2:1 at $\delta(^{11}B)$ = 13.0, −6.0, and −51.3. In the coupled ^{11}B NMR spectrum the resonance at $\delta(^{11}B)$ = −51.3 exhibits triplet character and is assigned to B(1). On the basis of relative intensities, the remaining resonances at $\delta(^{11}B)$ = +13.0 and −6.0 are assigned to the B(4) and B(3,5) atoms, respectively.

Bonding Patterns in Small Metallaboranes. The compounds reported in this investigation are unique, because they are the first metallapentaboranes prepared from $[B_4H_9]^-$. Also, the metals employed in this study bind to the B_4 ligands in ways that differ somewhat from the bonding exhibited in their complexes with other borane ligands. Therefore, it is of interest to consider the differences between the present examples and other previously reported metallaboranes.

For instance, a wide variety of borane to metal interactions are exhibited by iridaboranes. Direct metal to boron bonds are found in $[Ir(B_5H_8)Br_2(CO)\{P(CH_3)_3\}_2]$, which is formed from $[2\text{-}BrB_5H_8]$ and $[Ir^{I}Cl(CO)\{P(CH_3)_3\}_2]$.[25-27] The reaction involves an oxidative addition across the iridium complex by a B–Br bond. Oxidative addition across an iridium complex by a B–H bond has been shown to occur with large borane anions. These reactions are often accompanied by the loss of one of the neutral ligands from the iridium complex. For instance $[Ir(H)(\eta^3\text{-}B_9H_{13})(L)_2]$ can be prepared from the reaction between $[IrCl(CO)(L)_2]$ (L = $P(CH_3)_3$ or $P(C_6H_5)_3$) and $[B_9H_{14}]^-$, with CO being evolved.[28] Such a process is formally similar to the proposed oxidative addition across the Rh atom of $[RhCl\{P(C_6H_5)_3\}_3]$ by $[B_4H_9]^-$ in the formation of $[Rh(H)(\eta^3\text{-}B_4H_8)\{P(C_6H_5)_3\}_2]$. Once again such an oxidative addition is accompanied by the loss of a neutral ligand from the starting rhodium complex. By way of contrast, transfer of hydrogen from a borane anion to an iridium atom is observed in the reaction of $[IrCl(CO)\{P(C_6H_5)_3\}_2]$ with $[B_3H_8]^-$.[29] Here, however, in the resultant complex $[Ir(H)(\eta^3\text{-}B_3H_7)CO\{P(C_6H_5)_3\}_2]$ all the ligands of the starting

(24) Bushweller, C. H.; Beall, H.; Grace, M.; Dewkett, W. J.; Bilofsky, H. S. *J. Am. Chem. Soc.* **1971**, *93*, 2145.
(25) Churchill, M. R.; Hackbrath, J. J.; Davison, A.; Traficante, D. D.; Wreford, S. S. *J. Am. Chem. Soc.* **1974**, *96*, 4041.
(26) Marks, R. W.; Wreford, S. S.; Traficante, D. D. *Inorg. Chem.* **1978**, *17*, 756.
(27) Churchill, M. R.; Hackbrath, J. J. *Inorg. Chem.* **1975**, *14*, 2047.
(28) Boocock, S. K.; Bould, J.; Greenwood, N. N.; Kennedy, J. D.; McDonald, W. S. *J. Chem. Soc., Dalton Trans.* **1982**, 713.
(29) Greenwood, N. N.; Kennedy, J. D.; Reed, D. *J. Chem. Soc., Dalton Trans.* **1980**, 196.

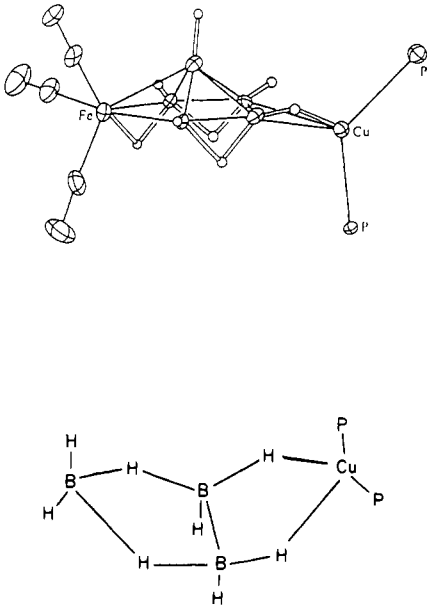

Figure 8. Molecular structures of $[Cu(B_3H_8)\{P(C_6H_5)_3\}_2]$[34] and $[Fe(B_5H_8)(CO)_3(\mu\text{-}Cu\{P(C_6H_5)_3\}_2)]$.[43]

material are retained on the metal. In the case of nido boranes two different modes of interaction are known. The first is the occupation of a bridging site as in $[\{Ir(B_6H_{10})_2Cl\}_2]$.[30] The second type of interaction is a multihapto one as in $[Ir(\eta^3\text{-}B_5H_8)(CO)\{P(C_6H_5)_3\}_2]$.[13] This is prepared from $K[B_5H_8]$ and $[IrCl(CO)\{P(C_6H_5)_3\}_2]$. Unlike the corresponding copper and nickel derivatives the iridium atom is not content to occupy a bridging proton site. An "oxidation insertion" by the iridium atom into $[B_5H_8]^-$ occurs. In most of the above examples where inclusion of the iridium atom into the borane framework has occurred, hydrogen bridge bonding from a boron atom to the metal is experienced, the prime exception being the borallyl $[B_3H_7]^{2-}$ complex.[29] Hence, the interaction of iridium with the anion $[B_4H_9]^-$ appears to be quite unlike any of the examples discussed above. A formal oxidative insertion into the borane framework can be viewed as having taken place. This has, however, occurred without hydrogen transfer from the borane ligand, without loss of ligands from the metal center, and without the formation of hydrogen bridge bonding with the borane ligand. All three of these conditions normally expected for such a metathetical reaction are exhibited by $[Rh(H)(\eta^3\text{-}B_4H_8)\{P(C_6H_5)_3\}_2]$.

The occupation of a bridging site is common for certain nickelaboranes, for example $[Ni(B_5H_8)Cl(PR_3)_2]$.[31] Nickel will also bond in a multihapto fashion with boranes. For instance nickel acts as a capping vertex in $[1\text{-}Ni(B_9H_9)(\eta^5\text{-}C_5H_5)]^-$.[32] In the case of the nickel tetraborane system, no isomer was found that contained nickel in a capping vertex site. With the exception of complexes of nickel with tetrahydroborate anion,[33] it is uncommon for nickel to undergo bridge bonding with hydrogen atoms in polynuclear metallaboranes. Hence, the existence of such a bonding scheme in $[2\text{-}NiB_4H_8\{(C_6H_5)_2P(CH_2)_2P(C_6H_5)_2\}]$ is unprecedented.

For cupraboranes, two distinct types of borane–metal interactions are noted, which are separate from that described for $[Cu(\eta^3\text{-}B_4H_9)\{P(C_6H_5)_3\}_2]$.[11] Typically with a nido borane a $[Cu\{P(C_6H_5)_3\}_2]^+$ electrophile will interact via bridge bonding and will occupy a proton bridging site. an example of this type of bonding arrangement is found with $[Cu(B_5H_8)\{P(C_6H_5)_3\}_2]$.[16] With the arachno borane anion $[B_3H_8]^-$, $[Cu(B_3H_8)\{P(C_6H_5)_3\}_2]$ is formed.[34-40] In this case the metal–borane interaction, Figure 8, is found to consist of two Cu–μ-H–B bridges. Hydrogen bridging is also found to be present in the salt $Cu_2B_{10}H_{10}$ and the complex $[Cu_2(B_{10}H_{10})\{P(C_6H_5)_3\}_4]$.[23,41,42] A form intermediate between these two extremes is present in the molecule $[Fe(CO)_3B_5H_8(\mu\text{-}Cu\{P(C_6H_5)_3\}_2)]$ formed via the anion $[Fe(B_5H_8)(CO)_3]^-$, which is strictly isoelectronic with $[B_6H_9]^-$.[43] Here the Cu atom occupies a bridging site, but unlike the *nido*-$B_5H_8^-$ derivative it is elevated from the plane of B–μ-H–B bonding, Figure 8. Also, the Cu atom participates in pseudobridge bonding with a terminal hydrogen atom. These structural types differ enormously from the η^3-bonding which is suggested for the Cu atom with $[B_4H_9]^-$. On would expect to see two or three Cu–μ-H–B bridging interactions as found for $[Cu(B_3H_8)\{P(C_6H_5)_3\}_2]$,[34-40] or $[Mn(CO)_3(B_3H_8)]$.[5]

In conclusion, the derivatives $[Ir(B_4H_9)(CO)\{P(CH_3)_2C_6H_5\}_2]$ and $[Cu(B_4H_9)\{P(C_6H_5)_3\}_2]$ adopt unusual and unexpected structures. The metallapentaboranes $[Ni(B_4H_8)\{(C_6H_5)_2P(CH_2)_2P(C_6H_5)_2\}]$ and $[Rh(H)(B_4H_8)\{P(C_6H_5)_3\}_2]$ adopt

Table III. Crystal Data

space group	$P2_1/c$
temp, °C	-162 ± 4
cell dimens	
a, Å	9.324 (2)
b, Å	23.162 (10)
c, Å	12.486 (3)
β,[a] deg	55.95 (1)
Z	4
V, Å^3	2198.5
d_{calcd}, g/cm^3	1.658
cryst size, mm	0.12 × 0.15 × 0.13
radiation	Mo Kα (0.710 69 Å)
linear abs coeff, cm^{-1}	61.99
diffractometer	Picker, four-circle
mode	θ–2θ
scan speed, deg/min	4.0
quadrants collected	$+h,+k,\pm l$
limits, deg	$5 < 2\theta < 50$
no. of total reflcns	4128
no. of total unique reflcns	3887
no. of total obsd reflcns	3159
R for averaging	0.034
final $R(F)$, $R_w(F)$	0.054, 0.050
goodness of fit	1.223

[a] The acute angle for β was inadvertently chosen early in the characterization and not noticed until refinement was complete. While the cell is thus nonstandard, the bond distances and angles are correct. The proper reduced cell is $a = 9.324$ (2) Å, $b = 23.162$ (10) Å, $c = 10.469$ (3) Å, and $\beta = 103.50$ (1)°. The reduced cell is related to the correct cell by using the matrix transformation $\{-1\ 0\ 0/0\ 1\ 0/1\ 0\ -1\}$.

(30) Davison, A.; Traficante, D. D.; Wreford, S. S. *J. Am. Chem. Soc.* **1974**, *96*, 2802.
(31) Greenwood, N. N.; Staves, J. *J. Chem. Soc., Dalton Trans.* **1977**, 1788.
(32) Leyden, R. N.; Sullivan, B. P.; Baker, R. T.; Hawthorne, M. F. *J. Am. Chem. Soc.* **1978**, *100*, 3758.
(33) Gilbert, K. B.; Boocock, S. K.; Shore, S. G. In "Comprehensive Organometallic Chemistry"; Wilkinson, G., Stone, F. G. A., Abel, E. W., Eds.; Pergamon Press: Oxford, 1982; Chapter 41.1, pp 910–911 and references therein.
(34) Lippard, S. J.; Melmed, K. M. *Inorg. Chem.* **1969**, *8*, 2755.
(35) Lippard, S. J.; Ucko, D. A. *Inorg. Chem.* **1968**, *7*, 1051.
(36) Klansberg, F.; Muetterties, E. L.; Guggenberger, L. J. *Inorg. Chem.* **1968**, *7*, 2272.
(37) Lippard, S. J.; Ucko, D. A. *Chem. Commun.* **1967**, 983.
(38) Bushweller, C. H.; Beall, H.; Dewkett, W. J. *Inorg. Chem.* **1976**, *15*, 1739.
(39) Beall, H.; Bushweller, C. H.; Dewkett, W. J.; Grace, M. *J. Am. Chem. Soc.* **1970**, *92*, 3484.
(40) Beall, H.; Bushweller, C. H.; Grace, M. *Inorg. Nucl. Chem. Lett.* **1971**, *7*, 641.
(41) Dobrott, R. D.; Lipscomb, W. N. *J. Chem. Phys.* **1962**, *37*, 1779.
(42) Paxson, T. E.; Hawthorne, M. F.; Brown, L. D.; Lipscomb, W. N. *Inorg. Chem.* **1974**, *13*, 2772.
(43) Magnion, M.; Ragaini, J. D.; Schmitkons, T. A.; Shore, S. G. *J. Am. Chem. Soc.* **1979**, *101*, 754.

Table IV. Positional Parameters for $[Ir(\eta^4\text{-}B_4H_9)(CO)\{P(CH_3)_2C_6H_5\}_2]$

atom	10^4x	10^4y	10^4z	atom	10^3x	10^3y	10^3z
Ir(1)	1370 (1)	1470.3 (2)	943.4 (4)	H(1)	492 (12)	131 (4)	−19 (9)
B(2)	4100 (16)	1593 (6)	316 (13)	H(2)	474 (15)	188 (5)	−79 (11)
B(3)	3362 (17)	2011 (7)	−572 (13)	H(3)	398 (22)	195 (8)	117 (17)
B(4)	2417 (15)	1494 (7)	−1126 (12)	H(4)	149 (11)	45 (4)	−68 (9)
C(6)	651 (15)	2104 (5)	2137 (10)	H(5)	374 (17)	55 (7)	−68 (13)
O(7)	278 (12)	2494 (4)	2785 (8)	H(6)	343 (16)	99 (6)	−176 (12)
P(8)	−1406 (3)	1444 (1)	1313 (2)	H(7)	369 (11)	182 (4)	−167 (8)
P(9)	1077 (4)	748 (1)	2387 (3)	H(8)	173 (12)	165 (4)	−158 (9)
C(10)	−2061 (17)	2149 (6)	1063 (13)	H(9)	332 (11)	250 (4)	−57 (9)
C(11)	−1739 (17)	979 (6)	267 (11)	H(10)	−127 (15)	222 (5)	44 (12)
C(12)	−3258 (13)	1264 (5)	2964 (10)	H(11)	−309 (11)	208 (4)	110 (8)
C(13)	6245 (15)	1651 (5)	3977 (11)	H(12)	−212 (14)	246 (5)	161 (11)
C(14)	−5151 (15)	1530 (6)	5248 (11)	H(13)	−285 (12)	104 (4)	47 (8)
C(15)	−6035 (15)	1018 (6)	5519 (11)	H(14)	928 (11)	110 (4)	936 (9)
C(16)	−5529 (14)	630 (6)	4492 (11)	H(15)	−155 (15)	58 (6)	31 (11)
C(17)	−4127 (15)	755 (5)	3214 (11)	H(16)	−318 (11)	200 (4)	388 (9)
C(18)	−165 (18)	113 (5)	2533 (13)	H(17)	−556 (17)	181 (6)	598 (13)
C(19)	3072 (18)	422 (6)	2044 (13)	H(18)	−717 (13)	97 (4)	647 (10)
C(20)	82 (14)	984 (5)	4090 (10)	H(19)	−640 (14)	24 (5)	488 (11)
C(21)	−1592 (15)	845 (5)	5068 (11)	H(20)	−365 (13)	44 (5)	252 (10)
C(22)	−2305 (16)	1029 (6)	6352 (12)	H(21)	−132 (18)	24 (6)	293 (13)
C(23)	−1320 (17)	1364 (5)	6654 (12)	H(22)	19 (14)	−13 (5)	180 (11)
C(24)	351 (16)	1506 (6)	5677 (12)	H(23)	−10 (13)	−18 (5)	318 (10)
C(25)	1037 (14)	1324 (5)	4393 (11)	H(24)	275 (12)	9 (4)	274 (9)
				H(25)	341 (18)	18 (7)	145 (15)
				H(26)	394 (24)	69 (8)	205 (18)
				H(27)	−206 (16)	64 (6)	498 (13)
				H(28)	−351 (11)	94 (4)	690 (9)
				H(29)	−180 (12)	144 (4)	764 (9)
				H(30)	121 (11)	178 (4)	594 (8)
				H(31)	222 (13)	144 (4)	375 (10)

a more regular geometry reminiscent of that found in $[2\text{-}CoB_4H_8(Cp)]$.[15]

Experimental Section

All transition-metal complexes used as starting materials were synthesized by literature methods;[44-47] the synthesis of the $[B_4H_9]^-$ ion has been described previously.[2,48] $1\text{-}MeB_4H_9$ was synthesized by a previously reported method.[49] All solvents were dried by standard procedures and stored in vacuo in bulbs.[50] THF and diethyl ether were stored over sodium benzophenone ketyl.

Structure Determination. A suitable crystal of $[Ir(\eta^4\text{-}B_4H_9)(CO)\{P(CH_3)_2C_6H_5\}_2]$ was obtained by cleaving a small nearly cubic fragment from a larger colorless needle. The crystal was mounted on a glass fiber by using silicone grease and cooled to −162 °C with a nitrogen boil-off cooling system.[14] The Picker diffractometer and experimental techniques used have been described previously.[51] A systematic search of a limited hemisphere of reciprocal space located diffraction maxima that could be indexed as monoclinic, with extinctions corresponding to the unique space group $P2_1/c$. Crystal and diffractometer data are summarized in Table III.

Data were corrected for Lorentz and polarization effects, and the structure was solved by a combination of direct methods and Fourier techniques.[52] All atoms were located, including hydrogens, and refined by full-matrix least-squares techniques (anisotropic for Ir, P, O, C, and B). Neutral-atom scattering factors were used,[53] and corrections for anomalous dispersion effects were included for all atoms.[53] Examination of ψ scans for several intense reflections indicated absorption corrections were not necessary, with random fluctuations of ~5% in the intensities. A final difference Fourier map contained three peaks of intensity 1.8–2.8 e Å^{-3} within 1.0 Å of the Ir atom and all other peaks of intensity less than 0.5 e Å^{-3}. Several of the hydrogen atom isotropic thermal parameters refined to negative values (the largest being −0.8 Å^2), although their positions seem well determined. A listing of atomic coordinates is given in Table IV.

Preparation of $[1,1,1\text{-}CO\{P(CH_3)_2C_6H_5\}_2\{Ir(\eta^4\text{-}B_4H_9)\}]$ (I). A two-necked vessel attached to an extractor was charged with KH (42 mg, 1.0 mmol) and sealed with a rotatable solid addition tube containing *trans*-$[IrCl(CO)\{P(CH_3)_2C_6H_5\}_2]$ (592 mg, 1.0 mmol). After evacuation on the vacuum line, B_4H_{10} (1.0 mmol) and $(CH_3)_2O$ (2–3 cm^3) were condensed into the reaction vessel at −196 °C. Stirring at −78 °C for 1 h afforded H_2 (0.96 mmol). $(CH_3)_2O$ was then distilled away at −78 °C, and THF (3 cm^3) and CH_2Cl_2 (5 cm^3) were added at −196 °C. The reaction mixture was allowed to warm to −23 °C for 2 h. During this time the solution changed color from a light green-yellow to a deep orange. The reaction mixture was then allowed to attain room temperature and was filtered to remove KCl (68 mg, 91%). The orange filtrate was reduced to dryness by removal of the THF and CH_2Cl_2. An orange gum resulted, which was dissolved in CH_2Cl_2 and applied in air to two 2 mm thick preparative-scale TLC plates (12 in. × 12 in.). The iridaborane was eluted with a 50:50 CH_2Cl_2/hexane mixture. The position of the iridaborane (R_f 0.40) was revealed by allowing the plates to briefly come into contact with iodine vapors. Bands containing the product were scraped from the plates and extracted with dry CH_2Cl_2 (50 cm^3).

The CH_2Cl_2 solution of $[Ir(\eta^4\text{-}B_4H_9)(CO)\{P(CH_3)_2C_6H_5\}_2]$ was filtered to remove silica gel and reduced to dryness in vacuo. The product was then recrystallized from dry pentane at −20 °C to give small needlelike crystals of the white $[Ir(\eta^4\text{-}B_4H_9)(CO)\{P(CH_3)_2C_6H_5\}_2]$, one of which was found to be useful for X-ray diffraction analysis. yield: 366 mg, 61%.

(44) Osborn, J. A.; Wilkinson, G. *Inorg. Synth.* **1967**, *10*, 67.
(45) Booth, G.; Chatt, J. *J. Chem. Soc.* **1965**, 3238.
(46) Davis, P. H.; Belford, R. L.; Paul, I. C. *Inorg. Chem.* **1973**, *12*, 213.
(47) Deeming, A. J.; Shaw, B. L. *J. Chem. Soc. A* **1968**, 1887.
(48) Johnson, H. D., II; Shore, S. G. *J. Am. Chem. Soc.* **1970**, *92*, 7586.
(49) Jaworisky, I. S.; Long, R. J.; Barton, L.; Shore, S. G. *Inorg. Chem.* **1979**, *18*, 56.
(50) Perrin, D. D.; Armagero, W. L.; Perrin, D. R. "Purification of Laboratory Chemicals"; Pergamon Press: Oxford.
(51) Huffman, J. C.; Lewis, L. N.; Caulton, K. G. *Inorg. Chem.* **1980**, *19*, 2755.
(52) All computations were performed on a CDC6600-CYBER172 multimainframe computer system using the Indiana University Molecular Structure Center XTEL program library. The XTEL library contains local code as well as programs from J. A. Ibers' Northwestern University program library and A. C. Larson's code from Los Alamos Scientific Laboratory.
(53) (a) Cromer, D. T.; Waber, J. T. "International Tables for X-ray Crystallography"; Ibers, J. A., Hamilton, W. C., Eds.; Kynoch Press: Birmingham, England, 1974; Vol. IV, Table 2.2A, p 72. (b) Stewart, R. F.; Davidson, E. R.; Simpson, W. T. *J. Chem. Phys.* **1965**, *42*, 3175–3187.
(54) Miller, V. R.; Grimes, R. N. *J. Am. Chem. Soc.* **1973**, *95*, 5078.

Preparation of *nido*-[2,2,2-(H){P(C$_6$H$_5$)$_3$}$_2$-{Rh(η^3-B$_4$H$_8$)}] (II). A two-necked reaction vessel attached to an extractor was charged with KH (23 mg, 0.50 mmol) and sealed with a rotatable solid addition tube containing [RhCl{P(C$_6$H$_5$)$_3$}$_3$] (476 mg, 0.51 mmol) in the drybox. After evacuation on the vacuum line, B_4H_{10} (0.50 mmol) and $(CH_3)_2O$ (1–2 cm^3) were condensed into the reaction vessel at −196 °C.

Stirring for 1 h at −78 °C afforded H_2 (0.50 mmol, 100% of theory). $(CH_3)_2O$ was distilled off at −78 °C, and THF (2 cm^3) and CH_2Cl_2 (2 cm^3) were condensed in at −196 °C. After [RhCl{P(C$_6$H$_5$)$_3$}$_3$] was tipped in, the reaction mixture was warmed to −18 °C and stirred for 3 h. Initially a clear orange solution was formed, followed by the precipitation of large quantities of a creamy white solid. Diethyl ether (6 cm^3) was condensed into the reaction flask at −78 °C, and the mixture was filtered at −78 °C. The filtrate was found to contain $P(C_6H_5)_3$ (118 mg, 92%). The isolated solids remaining on the frit were redissolved in CH_2Cl_2 (15 cm^3) at 0 °C, and the mixture was again filtered to remove KCl (30 mg, 81%; identified by X-ray powder diffraction). The filtrate was then concentrated by removal of CH_2Cl_2 (10 cm^3) at 0 °C, and $(C_2H_5)_2O$ (10 cm^3) was added at −78 °C to effect precipitation of the creamy white solid, which was isolated by filtration at −78 °C. Yield: 300 mg, 90%.

Anal. Calcd for $C_{36}H_{39}B_4RhP_2$: B, 6.36; C, 63.61; H, 5.78; Rh, 15.13. Found: B, 6.43; C, 63.41; H, 5.81; Rh, 14.82. IR spectrum (Nujol mull, cm^{-1}): 2555 (s), 2505 (s), 2495 (s), 2480 (s), 2300 (bw), 2230 (bw), 2160 (bw), 2070 (sm), 1810 (bm).

Preparation of [2,2-{(C$_6$H$_5$)$_2$P(CH$_2$)$_2$P(C$_6$H$_5$)$_2$}{Ni(η^3-B$_4$H$_8$)}] (III). A two-necked reaction vessel attached to an extractor was charged with KH (83 mg, 2.0 mmol) and [{(C$_6$H$_5$)$_2$P(CH$_2$)$_2$P(C$_6$H$_5$)$_2$}NiBr$_2$] (625 mg, 1.0 mmol) in the drybox.

After evacuation on the vacuum line, B_4H_{10} (1.0 mmol) and $(CH_3)_2O$ (2–3 cm^3) were condensed into the reaction vessel at −196 °C. Stirring at −78 °C for 1 h afforded H_2 (0.96 mmol). The $(CH_3)_2O$ was pumped away at −78 °C, and THF (7–8 cm^3) and CH_2Cl_2 (10–12 cm^3) were condensed in at −196 °C. After the nickel complex was tipped in, the reaction mixture was warmed to −45 °C for 3 h with stirring and then stirred at −78 °C for 1 week. Hydrogen (0.78 mmol) was measured by a Toepler pump, and the deep red-orange solution was filtered at −78 °C to remove the KBr (180 mg, 76%; identified by X-ray powder diffraction). The solvents were then distilled away from the red-orange product at 0 °C, resulting in the isolation of 600 mg of solid (mixture of starting material and product). The nickelaborane was purified by thin-layer chromatography in the drybox using 2 mm thick silica gel plates and a 70:30 CH_2Cl_2/hexane solvent system as the eluant. Hence, 150 mg (25%) of the pure orange [Ni(B$_4$H$_8$)(dppe)] was obtained.

Anal. Calcd for $C_{26}H_{32}B_4NiP_2 \cdot {}^1/_2CH_2Cl_2$: B, 7.80; C, 57.78; H, 5.04; Ni, 10.66. Found: B, 7.22; C, 57.50; H, 5.98; Ni, 10.36. IR spectrum (Nujol mull, cm^{-1}): 2550 (s), 2500 (s), 2440 (vs), 2380 (w), 2280 (bm), 2210 (w).

[Cu(η^3-B$_4$H$_9$){P(C$_6$H$_5$)$_3$}$_2$] (IV). Using [CuCl{P(C$_6$H$_5$)$_3$}$_3$]. In the drybox a two-necked reaction vessel attached to an extractor was charged with 1.0 mmol of KH and sealed with a rotatable solid addition tube containing 0.816 g of [CuCl{P(C$_6$H$_5$)$_3$}$_3$] (0.92 mmol).

After evacuation on the vacuum line, 1.0 mmol of B_4H_{10} and 1.2 mL of $(CH_3)_2O$ were condensed in at −196 °C. Stirring at −78 °C for 15 min afforded 0.96 mmol of H_2. $(CH_3)_2O$ was distilled off at −78 °C, and THF (7 mL) was condensed in at −196 °C. [CuCl{P(C$_6$H$_5$)$_3$}$_3$] was tipped in and 15 mL of CH_2Cl_2 condensed into the flask at −196 °C. The mixture was allowed to thaw and was stirred at −45 °C for 3 h and then at −78 °C overnight. Diethyl ether (24 mL) was condensed onto the reaction mixture at −78 °C while it was stirred, causing precipitation of large amounts of a creamy white solid. The mixture was then filtered at −78 °C. Isolated solids remaining on the frit were washed with cold $(C_2H_5)_2O$. The white precipitate was redissolved in 15 mL of CH_2Cl_2, and the mixture was again filtered cold to remove the byproduct KCl (identified by its X-ray powder diffraction pattern). The filtered solution was concentrated by removal of ~10 mL of CH_2Cl_2 at −23 °C. Diethyl ether (8 mL) was added at −78 °C to effect precipitation of the white product. This was isolated by filtration at −78 °C. The product, IV, was repeatedly washed with $(C_2H_5)_2O$ and then with pentane to remove any remaining $P(C_6H_5)_3$. Yield: 0.18 g, 30%. Calcd for $B_4H_{36}CuH_{39}P_2$: B, 6.75; C, 67.52; Cu, 9.92; H, 6.14; P, 9.67. Found: B, 6.81; C, 68.28; Cu, 10.08; H, 6.70; P, 9.00. IR spectrum (C_4Cl_6 mull, cm^{-1}): 2530 (s), 2464 (s), 2447 (s).

Using [CuBr{P(C$_6$H$_5$)$_3$}$_2$·$^1/_2$C$_6$H$_6$]. Into a two-necked reaction vessel containing 1.0 mmol of KH with 0.7426 g of [CuBr{P(C$_6$H$_5$)$_3$}$_2$·$^1/_2$C$_6$H$_6$] (1.05 mmol) in a side-arm tip-tube were distilled B_4H_{10} (1.05 mmol) and $(CH_3)_2O$ (1.2 mL) at −196 °C. Stirring at −78 °C for $^1/_2$ h yielded 0.96 mmol of H_2. $(CH_3)_2O$ was distilled off at −78 °C, and THF (7 mL) and CH_2Cl_2 (10 mL) were added at −196 °C. The copper complex was tipped into the solution of $K[B_4H_9]$ at −78 °C. The reaction mixture was stirred at −45 °C for 3 h and then at −78 °C overnight. Workup of the reaction mixture performed under conditions similar to those used above. The byproduct KBr (0.19 g, 92%) was isolated and identified by its X-ray powder pattern. Yield of [{(C$_6$H$_5$)$_3$P}$_2$Cu(η^3-B$_4$H$_9$)]: 0.341 g, 51%.

Anal. Calcd for $B_4C_{36}CuH_{39}P_2$: B, 6.75; C, 67.52; Cu, 9.92; H, 6.14; P, 9.67. Found: B, 7.04; C, 67.54; Cu, 10.34; H, 6.40; P, 9.03.

It was also possible to prepare [Cu(η^3-B$_4$H$_9$){P(C$_6$H$_5$)$_3$}$_2$] from the reaction between [CuCl{P(C$_6$H$_5$)$_3$}$_3$] and $K[B_5H_{12}]$.[2] Though in this case the yield was higher (~70%), the product was always heavily contaminated with equimolar amounts of $BH_3 \cdot P(C_6H_5)_3$.

Preparation of [2,2-{P(C$_6$H$_5$)$_3$}$_2$-{Cu(η^3-CH$_3$B$_4$H$_8$)}] (V). Dimethyl ether (0.65 mL) and 0.565 mmol of [1-MeB$_4$H$_9$] were condensed into a reaction vessel containing 0.50 mmol of KH at −196 °C. Stirring at −78 °C for 15 min afforded 0.50 mmol of H_2. The remaining volatile materials were removed at −78 °C. Under a flow of N_2 gas, 0.4429 g (0.50 mmol) of [CuCl{P(C$_6$H$_5$)$_3$}$_3$] was added to the reaction vessel, which was then attached to an extractor and evacuated. Tetrahydrofuran (1 mL) and CH_2Cl_2 (6 mL) were condensed in at −196 °C. The solution was stirred at −45 °C for 2 h and then at −78 °C overnight. An additional 8 mL of CH_2Cl_2 was added to dissolve the white slurry. Filtration at −50 °C isolated the byproduct KCl (identified by its X-ray powder pattern). Removal of the solvents from the filtrate yielded an off-white solid. This became clear white upon repeated washings with cold ether. Finaly yield of [{(C$_6$H$_5$)$_3$P}$_2$Cu(η^3-B$_4$H$_8$Me)]: 0.24 g, 73%.

Acknowledgment. We thank the Army Research Office and the National Science Foundation for generous support of this work through Grants DAA G29-82-K-0112 and CHE 79-18149. Certain of the FT NMR spectra were obtained with the aid of Dr. C. E. Cottrell at The Ohio State University Chemical Instrument Center (funded in part by National Science Foundation Grant CHE-7910019).

Registry No. I, 91491-95-1; II, 91491-96-2; III, 91491-97-3; IV, 69680-95-1; V, 91523-00-1; *trans*-[IrCl(CO){P(CH$_3$)$_2$C$_6$H$_5$}$_2$], 21209-82-5; [RhCl{P(C$_6$H$_5$)$_3$}$_3$], 14694-95-2; [{(C$_6$H$_5$)$_2$P(CH$_2$)$_2$P-(C$_6$H$_5$)$_2$}NiBr$_2$], 14647-21-3; [CuCl{P(C$_6$H$_5$)$_3$}$_3$], 15709-76-9; [CuBr{P(C$_6$H$_5$)$_3$}$_2$·$^1/_2$C$_6$H$_6$], 36273-10-6.

Supplementary Material Available: Tables of anisotropic thermal parameters, isotropic thermal parameters, least-squares plane data, and F_o and F_c (27 pages). Ordering information is given on any current masthead page.